

Global nucleosome dynamics in yeast

Cornelia Amariei

1 Introduction

A deeper understanding of the cellular dynamics and the transcription regulation are one of the central goals of modern biology. In eukaryotic cells, chromatin structure has been shown to be a highly dynamic property, which regulates essential cellular functions, such as gene transcription, DNA replication and repair. Chromatin is an array of nucleosomes formed by 147 bp of DNA which are wound around a histone octamer containing two copies of each core histone proteins H2A, H2B, H3 and H4, or, alternatively, from histone variants that specialize chromatin at particular regions. This packaging has a structural role, by allowing compaction of DNA in the nucleus, but has a repressive effect on transcription, since it hinders the binding of transcription factors and transcriptional machinery to gene promoters and coding regions.

Nucleosomes exhibit at least three dynamic properties *in vivo*: repositioning (that is, altering the position of the nucleosome on the DNA), compositional alteration (such as the replacement in *S. cerevisiae* of H2A histone with its variant, Htz1) and covalent modification (modifications of individual residues of histones). These dynamic properties are mediated by nucleosome modifying and nucleosome remodeling complexes, which work in concert to regulate the local and global properties of chromatin[1, 2]. Histone covalent modifications in particular have been the focus of many recent studies, which have revealed that the acetylation, methylation, phosphorylation, ubiquitination and sumoylation of the core histones have a crucial role in dynamically regulating gene activity[3, 4, 5, 6].

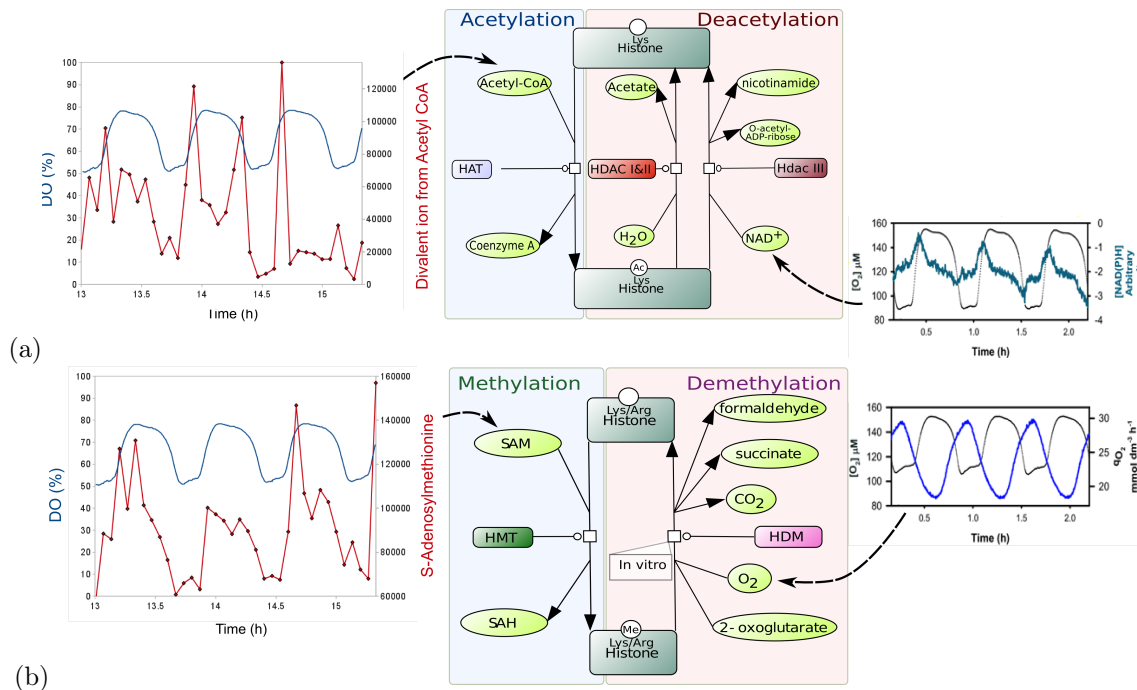


Fig. 1.1: Metabolic regulation of histone modifications. The known covalent histone modifications are conditioned by the availability of certain currency metabolites, which have been monitored online (NAD(P)H, O₂) or measured by CE-MS (Acetyl-CoA, SAM), revealing strong oscillatory patterns; (a) Acetylation (b) Methylation enzymatic reactions.

It has been postulated that the histone modification events are dependent on the availability of the “currency metabolites”[7] *in vivo*, such as acetaldehyde (precursor of acetyl-CoA required for acetylation - fig. 1.1a), and H₂S (precursor of S-adenosyl methionine required for methylation - fig. 1.1b), and that chromatin dynamics are therefore interwoven with cellular metabolism[8, 9, 10].

For the study of the dynamic correlation between the metabolic state, chromatin state and transcription regulation, *S. cerevisiae* grown in continuous culture represent an ideal organism, since they can be grown in precisely controlled conditions, can be easily manipulated and, under many conditions, the individuals auto-synchronize to produce a temperature-compensated oscillation, that involves respiratory switching between high respiratory activity (oxidative phase) and low respiratory activity (reductive phase). These metabolic oscillations can be conveniently tracked by on-line measurements, such as dissolved oxygen, NAD(P)H and H₂S. Moreover, it was shown that many core metabolites, as well as mRNA concentrations (fig. 1.2), oscillate with phase relationships to this respiratory cycle[11, 12].

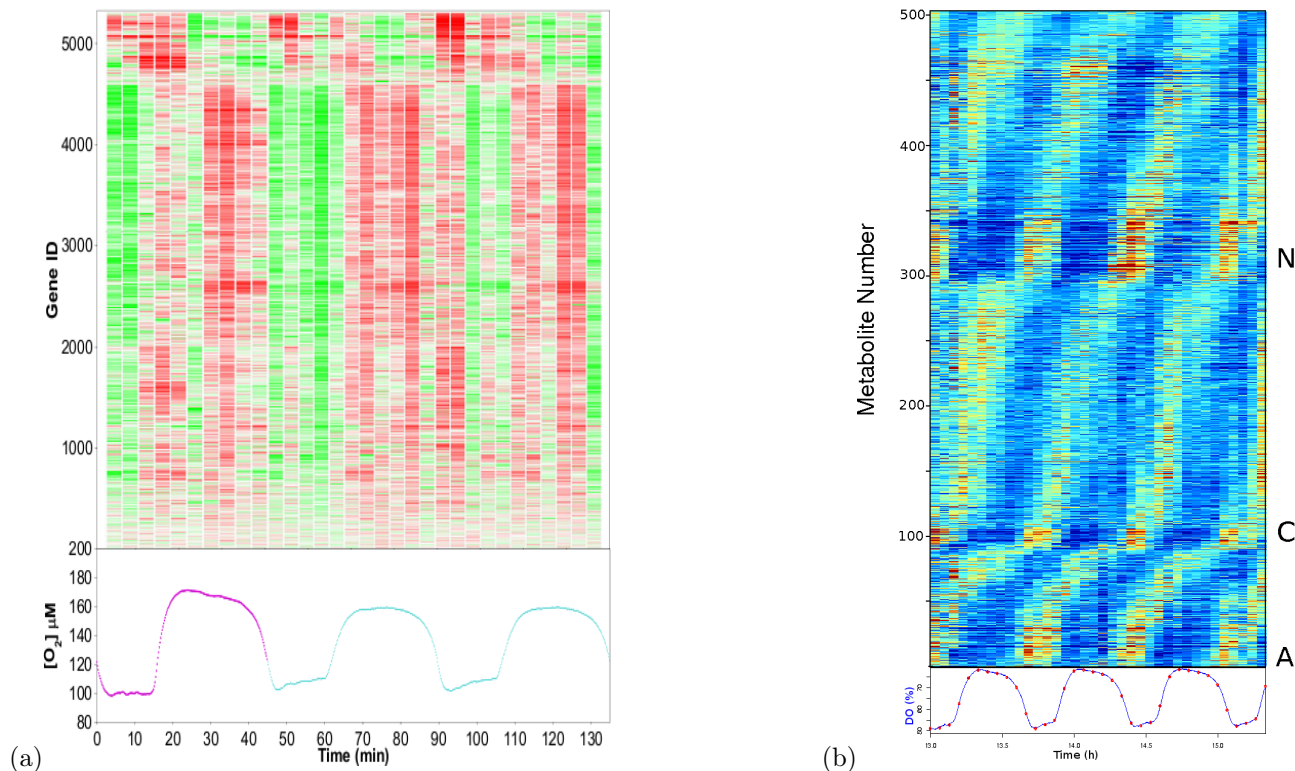


Fig. 1.2: Waves of transcription and metabolite production. (a) A heatmap of scaled GenechipTM expression data[13] from 32 microarrays show >90% of transcripts show oscillatory dynamics and their maximum production has distinct phase relationships with respiratory activity. Green represents scaled expression < 0.33 and red represents scaled expression > 3. The lower graph shows dissolved oxygen concentration for the experiment where the magenta line depicts the concentrations of the first 10 microarrays and the cyan line the last 22. The samples from these were taken 3 months apart.

(b) A contour plot of scaled CE-MS metabolite data show that ~500 peaks show oscillatory dynamics and have a similar production structure to transcription. Green represents scaled expression < 0.33 and red represents scaled expression > 3. The lower graph shows dissolved oxygen concentration (black; uM) and loess smoothed fluorimeter signal NAD(P)H (dark cyan; V). C represents cation, A anion and N nucleotide.

Essential cellular substrates with redox activity, such as the above mentioned S-adenosyl methionine and acetyl-CoA have been implicated in the synchronization of the respiratory oscillation[14, 15]. It is also likely that energetics (e.g., ATP:ADP) play a key role in the global regulation of transcript level, since nucleosome remodeling and several histone modification events are ATP-dependent. Generally, the role of these metabolites is often overlooked in global regulation, perhaps due to measurement difficulties. Recently, a Discrete Fourier Transform analysis method (Machne and Murray, in review) was used on two oscillatory transcriptome sets to define 7 consensus clusters of gene expression (4 major clusters and 3 transitional clusters, fig. 1.3). A functional analysis of these clusters revealed that genes expressed during the oxidative phase are involved in cell growth and anabolism, while the genes expressed in the reductive phase are involved in mitochondrial growth and catabolism. When compared with a large compendium of high-throughput data, differential promoter structures and nucleosome occupancy patterns (and the energetic requirements for remodeling) were implicated in temporal cluster development, pointing to an unknown energy-dependent, nucleosome-mediated mechanism regulating the transcriptional program.

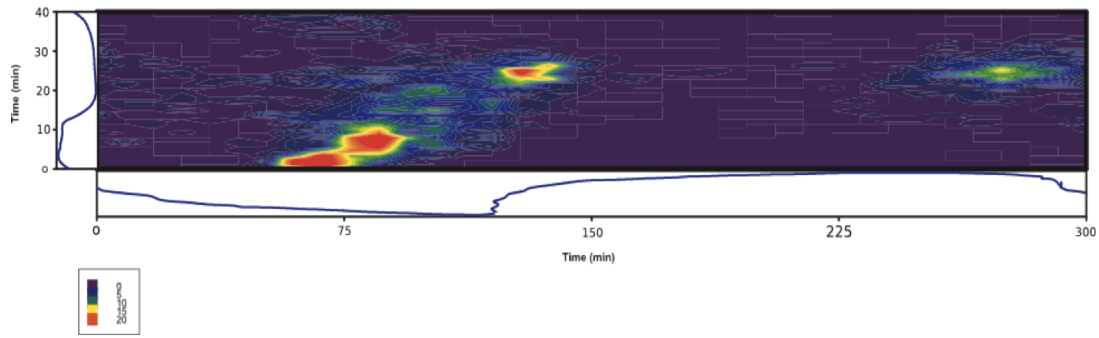


Fig. 1.3: A comparison between two oscillatory transcriptome datasets([16, 17]) with different oscillation periods (40 min and 300 min, respectively). The numbers on the legend refer to the numbers of genes expressed in a particular timeframe. The blue traces at the left and bottom of the image represent the DO trace in each system. We can observe 4 major clusters of genes, named A,B,C and D from left to right. A and B are expressed during the oxidative phase of the respiratory cycle, while C and D (that are expressed simultaneously in the 40 min oscillation) occur during the reductive phase.

1.1 Objectives

We are aiming at building a model of the dynamic relationship between metabolic state, chromatin state and transcription, both computationally and experimentally.

1. Obtain experimental data on the nucleosome positioning dynamics during the respiratory cycle and investigating the dependency on cellular energetics.
2. Obtain experimental data on histone modification dynamics and the dependency on core metabolism (e.g. currency metabolites).
3. Integrate this data into existing computational models of the core metabolism.
4. Integrate these results with previous experimental and computational data on transcription dynamics to construct a model of the metabolic feedback on transcription through chromatin structure dynamics that amenable to mathematical modeling.

1.2 Methodology

Microarray analysis of purified nucleosomal DNA time-series will be used for constructing a global, mono-nucleosome resolution map of the nucleosome dynamics. The relationship with cellular energetics will be studied by correlating the results with pre-existing time-series metabolome datasets (focusing on redox and ATP:ADP ratio), and by chemical perturbations known to affect cellular energetics (e.g. acetaldehyde, potassium cyanide). Histone modification dynamics will be studied through ChIP-qPCR and/or ChIP-seq time-series experiments against a multitude of histone modifications and histone variants. This data will be correlated with the known temporal profiles of the co-enzymes (e.g. acetyl-CoA, S-adenosyl methionine) and metabolites (e.g. acetate and H₂S) required for histone modifying activities, and their dependency can similarly be studied by chemical perturbations that affect the activity of histone-modifying enzymes.

The experimental results on chromatin dynamics and transcriptional dynamics will be analysed using an R package based on Discrete Fourier Transform-based methods that is being developed in our group. The results will be integrated in existing mathematical models of the yeast metabolism.

1.3 Anticipated result

From the previously mentioned study (Machne and Murray, in review), we know that two different remodeling complexes - RSC and Isw2 - that have a positive and negative effect on gene transcription respectively, were each shown to preferentially act on different gene clusters: the genes expressed in the oxidative phase were linked to RSC activity, while genes expressed in the reductive phase were linked to Isw2.

Our hypothesis is that nucleosomal repositioning events occur all throughout the genome during the oxidative phase, when the availability of ATP is at its highest, but has different effects on the transcription of different gene groups due to their differential promoter structure. Genes expressed in the oxidative phase (anabolic genes) commonly have nucleosome-free promoter regions (maintained by RSC complexes), and are thus easily accessible

for transcription when the energy required is available. Genes expressed in the reductive phase (catabolic genes) are subject to Isw2 remodeling activity when energy is available, resulting in their inhibition (fig. 1.4).

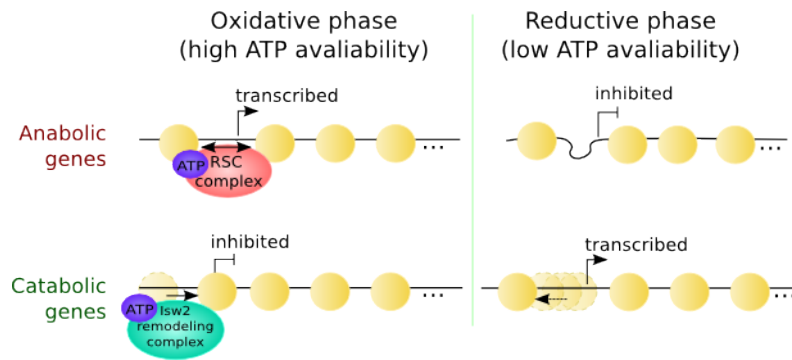


Fig. 1.4: Conceptual model of the differential energy-dependent transcription activation on oxidative and reductive genes. Anabolic genes are transcribed during the oxidative phase due to the ATP-dependent RSC complex activity, that may act as a “spacer” for maintaining the promoter accessibility. Catabolic genes are transcriptionally inhibited during the oxidative phase due to the Isw2-dependent addition/sliding of nucleosomes onto the promoter region. When ATP becomes unavailable, during the reductive phase, the loss of RSC activity may diminish the promoter accessibility for anabolic genes which become inhibited, and the loss of Isw2 activity on catabolic genes results in nucleosomes sliding in their “preferred” position, exposing the promoter region and thus being transcribed.

Furthermore, we expect to identify other metabolic bottlenecks involved in histone modification events to have similar global effects on the transcriptional activity.

Altogether, our data will provide a simplified view of the global transcriptional regulation driven by the energetic state of the cells attenuating chromatin structure.

2 Progress

2.1 ChIP-qPCR analysis of chromatin dynamics

We have conducted a series of Chromatin Immunoprecipitation experiments on time-series samples, aimed at better understanding the dynamics of the transcription regulation with regard to histone positioning and modifications. Although the results are still preliminary and further work is needed, they suggest that:

- the waves of mRNA quantities shown in previous studies are indeed regulated at transcriptional level;
- histone acetylation shows differences over the respiratory cycle and correlates with differentially expressed genes
- mass nucleosome repositioning may be a global dynamic property over the respiratory cycle that occurs during the oxidative phase.

2.1.1 Polymerase II binding correlates with mRNA temporal profile

As a first experiment, we wanted to confirm that the oscillatory patterns in mRNA profiles from previous microarray time-series experiments ([13]) were regulated at a transcriptional level and not exclusively related to mRNA stability, degradation, etc. We therefore performed ChIP experiments against PolII on 14 successive timepoints (one respiratory cycle) and used the resulting DNA for qPCR with four primer sets corresponding to the coding regions of four genes that had shown strong oscillations in the microarray dataset. Two of these genes (NOP1 and SAM1) were shown to peak in the oxidative phase, while the other two (MRH1 and ACA1) were shown to peak at the end of the reductive phase (see fig. 2.1). For normalizing the results, we used a primer set corresponding to a telomeric region on chromosome VI that is considered not to be transcribed. The results (fig. 2.2a) show a strong correlation to the microarray data: PolII is found bound on NOP1 and SAM1 at high levels during the oxidative phase, when the number of transcripts of these genes are at their highest. PolII binding to MRH1 and ACA1 occurs mostly at mid-reductive phase and shows broader peaks, relating very well with the mRNA data which shows the highest mRNA concentration increase for these genes in mid-reductive phase. Statistical analysis of these results show that the correlations between the genes in oxidative phase and reductive phase respectively are significant (fig. 2.2b).

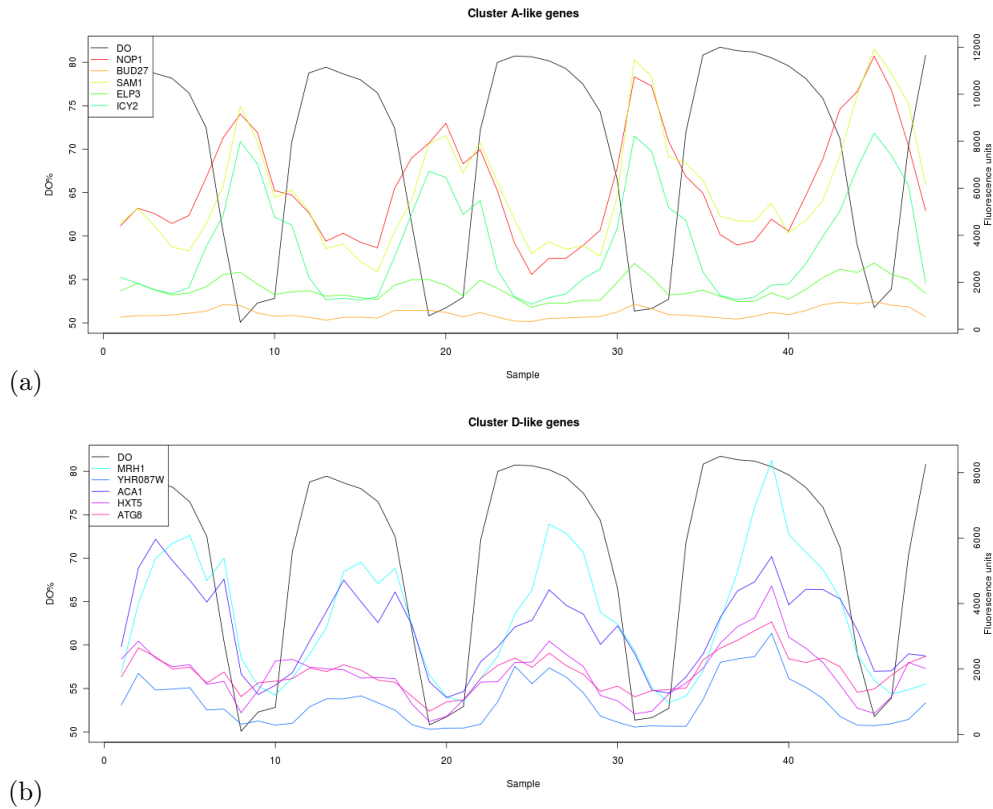


Fig. 2.1: Microarray time-series experiment (from[13]): (a) shows the expression profile of several genes peaking in the oxidative phase, while (b) shows the expression of genes in reductive phase relative to dissolved oxygen traces.

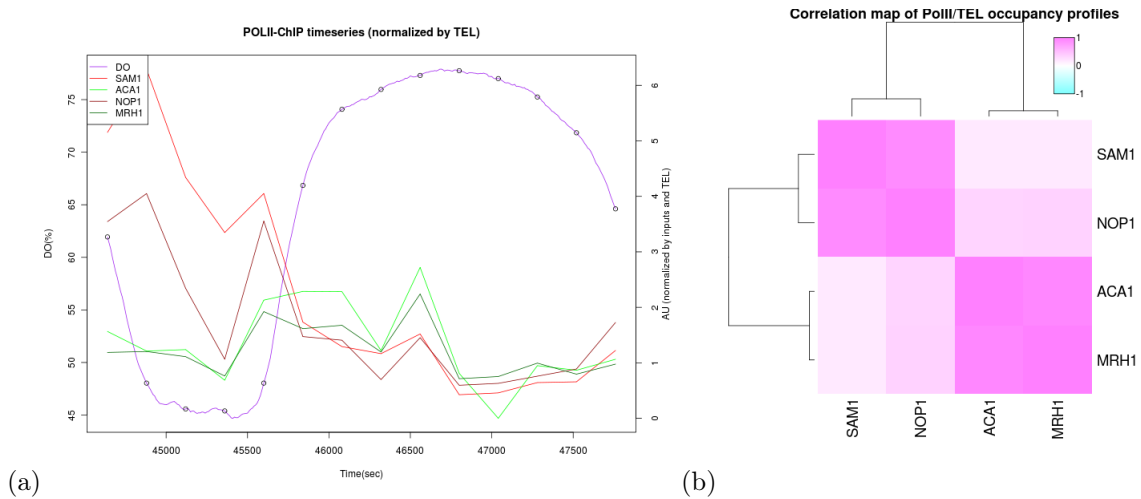


Fig. 2.2: qPCR experiments on anti-Pol II ChIP time-series. (a) Temporal profile of the Pol II binding at the promoter of 2 genes expressed in oxidative phase (in red) and 2 genes expressed in reductive phase (in green). The values were normalized by total chromatin control and telomeric region qPCRs. Circles on the DO trace show sampling times. (b) Correlation map. The values represent correlation coefficients; ACA1-MRH1 and SAM1-NOP1 correlations are statistically significant (p -values: $6.787e-07$ and $7.558e-06$ respectively).

2.1.2 Nucleosome repositioning and histone modification upstream of TSS

We continued this study by looking for differences in histone modifications between the two groups of genes that were shown to be differentially transcribed. We therefore performed ChIP against an acetylated site on histone H3 (H3K9) and against histone H3. Since nucleosome-mediated transcriptional control is considered most prominent on the promoter region, the qPCR experiments were done using primers around the -100 bp

region relative to the transcriptional start site (TSS).

As a first result, histone H3 (and presumably the whole nucleosome) closest to the transcription start site seems to be displaced during the oxidative phase at all promoters and then repositioned towards late reductive phase (fig. 2.3a). There is no statistical difference between the two groups of genes, suggesting that nucleosome positioning upstream of TSS is not related to the differential expression of these groups of genes (fig. 2.3b).

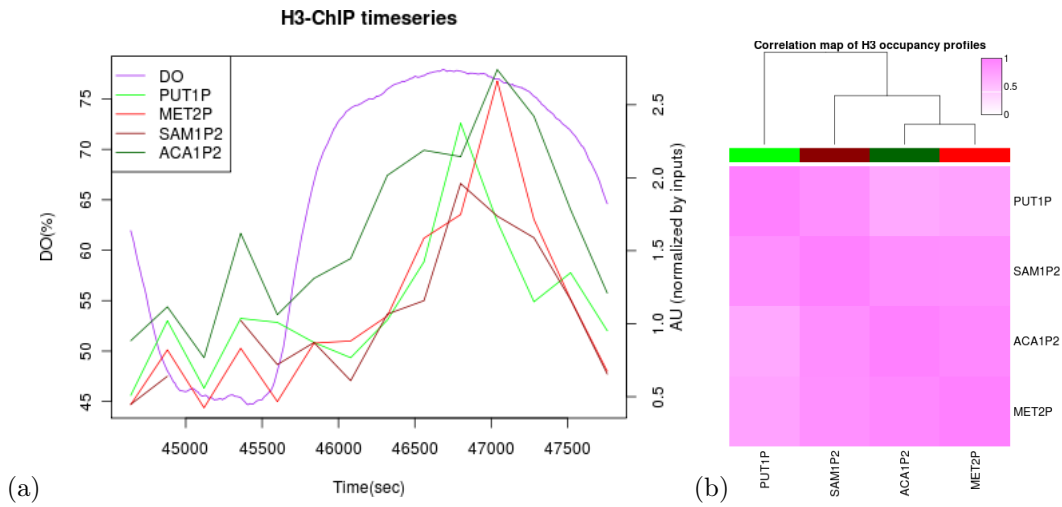


Fig. 2.3: qPCR experiments on anti-H3 ChIP time-series. (a) Temporal profile of the H3 occupancy at the promoter of 2 genes expressed in oxidative phase (in red) and 2 genes expressed in reductive phase (in green). The values were normalized by total chromatin control. (b) Correlation map showing no statistical difference between the two gene groups. The values represent correlation coefficients.

The anti-H3K9acetyl ChIP experiments also showed a strong correlation between different promoters. and, more interestingly, reveal acetylation “spikes” during the respiratory cycle (fig. 2.4a). However, since we had no control with which to normalize the data, these results may simply be due to technical errors and require further confirmation. On the other hand, unlike anti-H3 ChIP results, this dataset shows a clear correlation with the gene expression groups: the genes that are coexpressed also show higher similarity in H3K9 acetylation profiles, suggesting that acetylation is linked to differentially expressed groups of genes (fig. 2.4b).

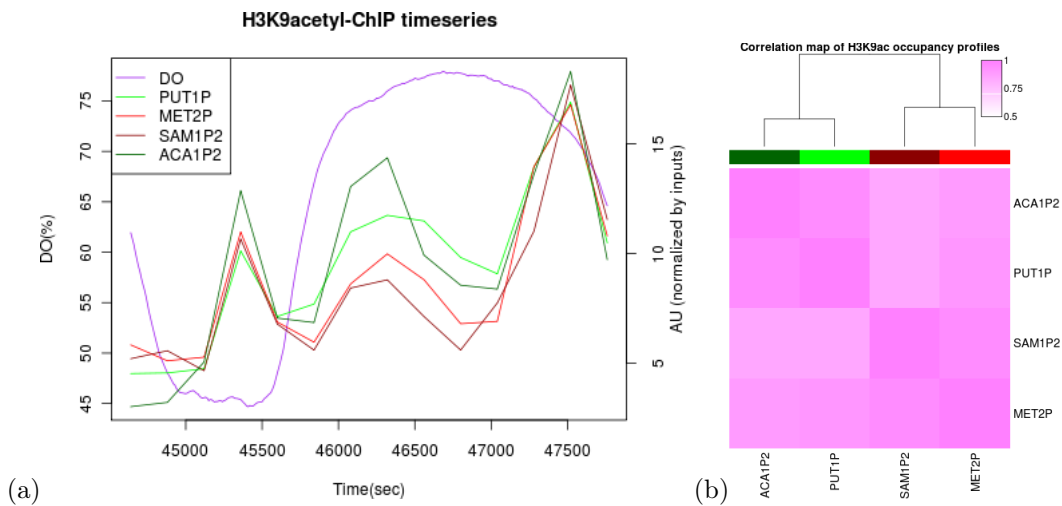


Fig. 2.4: qPCR experiments on anti-H3K9acetyl ChIP time-series. (a) Temporal profile of the H3 occupancy at the promoter of 2 genes expressed in oxidative phase (in red) and 2 genes expressed in reductive phase (in green). (b) Correlation map showing a slight difference in the profile of the two gene groups, which is likely masked by the global nucleosome enrichment. The values represent correlation coefficients.

2.1.3 Nucleosome repositioning along the gene

The 40-time-point time-series qPCR-ChIP experiments using anti-H3 antibody and amplifying a 100 bp region around TSS of Lys20 has shown the previously-observed pattern; The qPCR results showed a reproducible

increase in DNA during reductive phase compared to the oxidative phase (fig.2.5a). The qPCR conducted with the same primer set on the sheared chromatin (before immunoprecipitation) resulted in a noisy signal (fig. 2.5b) that did not show a statistical correlation with the qPCR-ChIP (correlation coefficient = 0.3416453).

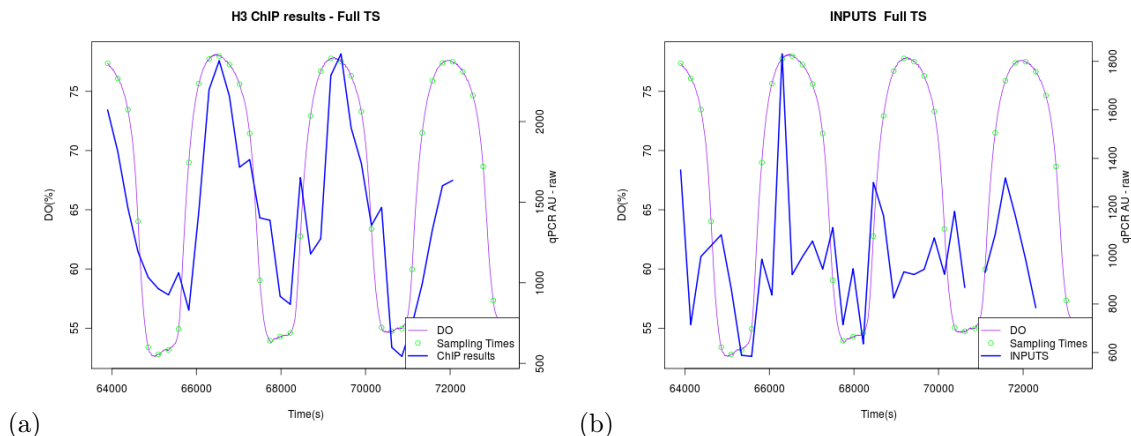


Fig. 2.5: qPCR experiments on (a) anti-H3 ChIP (b) input chromatin extract time-series on the promoter region of Lys20. Circles on the Dissolved oxygen (DO) trace show sampling times.

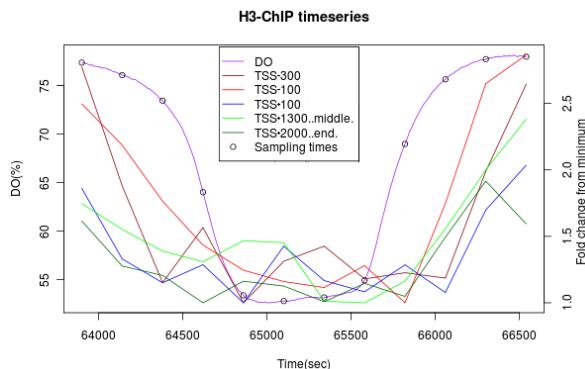


Fig. 2.6: Anti-H3 ChIP-qPCR time-series along the gene Lys20 at 5 different putative nucleosome regions.

To observe the DNA occupancy along the gene, we have repeated the qPCR experiments on the first respiratory cycle, using primers amplifying several locations along one gene: from the putative nucleosome positions around and on the transcription start site, the middle and the end of the gene. This experiment has shown that the enrichment during reductive phase occurs at all tested positions, but vary in amplitude (fig. 2.6).

2.2 Microarray analysis of global nucleosome dynamics

Although the ChIP-seq experiments on H3 were encouraging, the chromatin for these experiments has been fragmented by sonication that typically yields fragments of 300-1000 bp. In order to improve the resolution of the nucleosome occupancy, we have steered away from mechanical disruption methods and opted for enzymatic methods of cell disruption and DNA shearing. We have adapted and improved the existing methods to obtain a highly-reliable, quick mononucleosomal DNA purification method for time-series, which is described in the methods section.

Using this method we have extracted mononucleosomal DNA as well as genomic (control) DNA from a time-series of 40 samples, over 3 respiratory cycles (fig. 2.7).

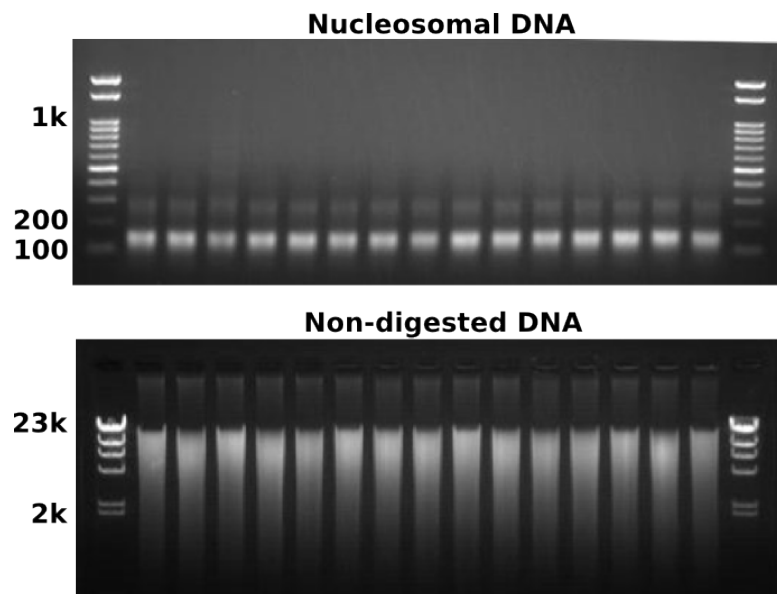


Fig. 2.7: Agarose gel of the first 15 samples from the time-series of nucleosomal (top) and genomic DNA (bottom) extracted using our method.

The obtained DNA was quantified using Hoechst dye and suggest the nucleosomal DNA extracted accounts for about half of the total DNA (fig. 2.8). Also, there appears to be an oscillation dependent variation of genomic DNA that may relate to the S-phase or different states of chromatin packaging.

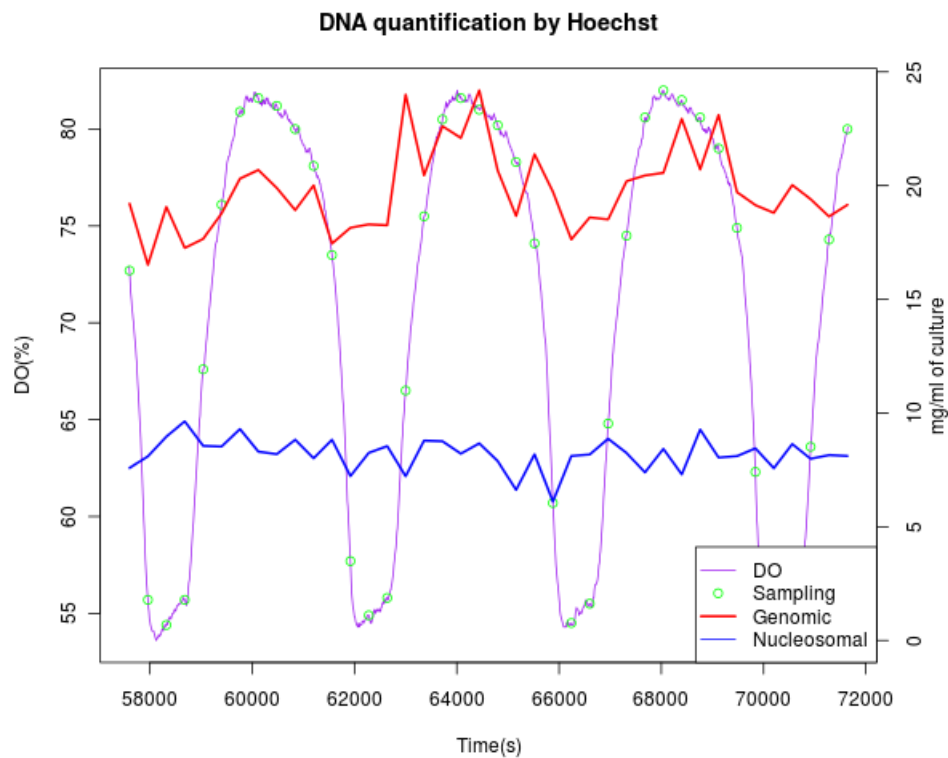


Fig. 2.8: Hoechst dye quantification of the extracted DNA.

We have then performed a qPCR assay as previously described using the primers for the Lys20 promoter region. Results show a high similarity with the previous H3 ChIP-qPCR test, confirming these results and the reliability of our method (fig. 2.9).

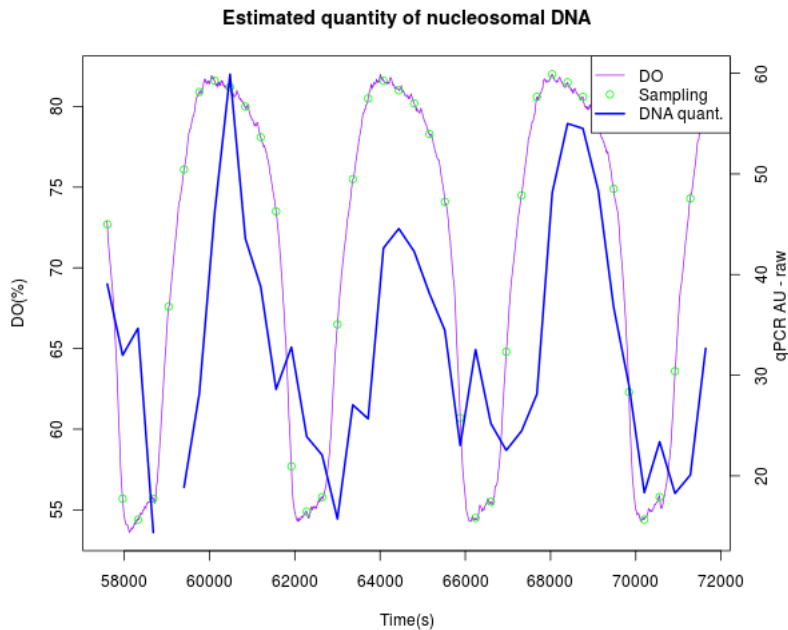


Fig. 2.9: qPCR assay on the nucleosomal DNA samples using a primer on the promoter region of *Lys20*. Circles on the Dissolved oxygen (DO) trace show sampling times.

The samples were then labeled using a dual-color kit and analysed on custom-made tiling arrays. We are processing the data obtained and the resulting dataset will be analyzed with software developed within our group in order to identify the global nucleosome repositioning events and their correlation with previous transcriptome and metabolome datasets.

2.3 Materials and Methods

2.3.1 Culture growth and sample preparation

The *S. cerevisiae* strain used was IFO0233 and was grown in continuous culture as described in [14]. A total of 40 samples were taken 4 minutes apart over approximately 3 respiratory cycles. Samples of 1 ml were fixed in 1% formaldehyde, placed on rotator for 12 minutes, neutralized with 0.1 volume of 2M glycine and placed on rotator for another 12 minutes. Samples were then spun down for 1 min on a table-top centrifuge and the supernatant was discarded. The pellets were stored at -80C.

2.3.2 Chromatin Immunoprecipitation and qPCR

For ChIP experiments, the frozen pellets were thawed on ice, washed in FA-Lysis buffer, resuspended in 700 μ l of the same buffer and disrupted by bead-beating, using 0.5 mm diameter glass beads and beat for 5x30 seconds with 1 minute cooling breaks on ice. After removing the beads, 150 μ l of the cell lysate was diluted in FA-Lysis buffer to a volume of 1.5 ml and sonicated for 15 min (cycles of 30 sec. on and 30 sec. off). Finally the sonicated samples were centrifuged twice and the final supernatant - the chromatin extract - was stored at -80C.

For each ChIP, we transferred 75 μ l of chromatin extract and 225 μ l FA-Lysis buffer to a non-stick microcentrifuge tube and incubated with 2 μ l of antibody for 3h to overnight at 4C on a rotary wheel. The IP reaction was centrifuged for 10 min at 4C and the supernatant was transferred to a Spin-X column containing 30 μ l of protein A agarose slurry (pre-incubated with 1 mg/ml BSA; Pierce). The samples were incubated for 2h at 4C on a rotary wheel and centrifuged at 3200 rpm for 2 minutes. The eluate was discarded and the column was washed sequentially (5 minutes each) with 700 μ l of FA-Lysis buffer, FA500, LiCl wash solution and TES. Finally, the column was transferred to new microcentrifuge tube and incubated at 37C for 30 minutes with agitation after adding 100 μ l of elution buffer. The sample was eluted by centrifugation at 9000 rpm for 2 min and treated with Proteinase K (20 μ g in 100 μ l of water; Roche) at 65C overnight. Finally, the sample was purified using the QIAquick PCR purification kit (Qiagen) following the manufacturer instructions. The resulting DNA samples were stored at -20C. For total chromatin control samples (inputs), 0.75 μ l of chromatin extract was mixed with 100 μ l of elution buffer, treated with Proteinase K and purified as described above. The antibodies used were: anti-PolIII (Abcam, ab5408), anti-H3 (Abcam, ab1791) and anti-H3K9acetyl (Millipore 07-352).

For PCR reactions, 2 μ l of each DNA sample was amplified by real-time PCR using Absolute QPCR SYBR green reagents (Abgene).

2.3.3 Gene and Primer pair selection

Starting from bioinformatic analyses of oscillatory expression sets, that have derived the top oscillatory genes (containing ~5500 genes), provided by R. Machne and D.B. Murray, we have selected the genes that meet the following criteria:

- High signal-to-noise ratio (>10)
- Gene length > 900 bp (ensuring a length sufficient for containing at least 5 nucleosomes)
- Oscillation amplitude in the top quartile

After this screening, we were left with ~200 genes, which we then clustered according to when their expression peak occurs and manually selected the genes with the sharpest expression peaks in each cluster, to a total of 20 genes. For these top genes we have then extracted the putative nucleosome positions from the *S. cerevisiae* genome-wide nucleosome nomenclature (<http://refnucl.atlas.bx.psu.edu>) and generated nucleosome-targeted primer pairs using Primer3 (<http://primer3.sourceforge.net>) and R (<http://cran.r-project.org>). From the resulting dataset, we then finally selected the genes for which we could generate primers for at least 4-5 regions of interest: the nucleosome on and around the TSS, the middle and the end of the gene. The selected genes were: Aca1, Lys20, Pck1, Met2, Thi6 and Str3. Out of these, for the current experiments, we only used the primers designed for Lys20.

2.3.4 Nucleosomal DNA purification and quantification

Crosslinked samples were thawed on ice, washed twice in 1ml TBS and pelleted at 12000xg, 4C, 2 min. The pellets were resuspended in 500 μ l of Zymolyase digestion solution (50 mM Tris-HCl pH. 7.4, 0.07% 2-me and 1000 U/ml of Zymolyase 100T (Seigaku corp.)) and incubated on rotator at room temperature for 1h. then supplemented with 0.1% Igepal, 200 μ M spermidine, 50 mM NaCl, 5 mM MgCl₂, 1mM CaCl₂, 5 μ l RNase A and 150U MNase (Wako), incubated at 37C for 30 minutes. Samples were swiftly transferred on ice and digestion was stopped with the addition of 0.01M EDTA and 0.05% SDS. Following a centrifugation step at 12000xg, 4C, 10 minutes, the supernatants were transferred to a new tube containing 10 μ l Proteinase K (20 μ g in 100 μ l of water; Roche) and incubated at 65C overnight.

The samples were cleaned using the standard phenol-chloroform-IAA protocol and phase-lock tubes. The aqueous phase was mixed with 2 volumes of EtOH, 0.04 volumes of glycogen, 0.04 volumes of 5M NaCl and centrifuged at 12000xg, room temperature, for 30 minutes. Supernatant was discarded and pellet was washed twice with 1 ml 80% EtOH. The pellet was then resuspended in 100 μ l water and purified using QIAquick PCR purification kit (Qiagen) according to instructions. The final samples were eluted in 100 μ l nuclease-free water and stored at 4C.

The control genomic DNA samples were prepared in parallel with the nucleosomal chromatin, by omitting the addition of MNase and salts (NaCl, MgCl₂, CaCl₂) during the digestion step.

For quantification, 0.5 μ l of each sample was dissolved in 99.5 μ l of Hoechst solution (Hoechst 33258 (Dojindo, Japan) 0.1 μ g/mL, Tris base 10 mM, Na₂EDTA 1 mM and NaCl 200 mM), loaded on a 96-well plate and read using a multi plate reader with excitation filter at 360 nm and emission filter at 460 nm. The DNA concentration was calculated relative to a ladder of HIND III digest of phage lambda DNA with known concentrations.

2.3.5 Sample labeling and microarray hybridization

For each set of samples (nucleosomal and genomic), an equal amount of each sample was used for labeling. This volume was calculated as the average of the highest quartile of the volume corresponding to 1 μ g of DNA in each set, ensuring that most samples will have over 1 μ g of DNA. Sample labeling was done using the Dual-Color DNA labeling kit (NimbleGen), according to manufacturer instructions. Genomic samples were labeled with Cy5 and nucleosomal samples were labeled with Cy3.

The resulting samples were then analysed on custom-made tiling arrays. The hybridization, washing and scanning of the arrays was performed according to the NimbleGen Array user manual for ChIP-chip Analysis.

References

- [1] Bradley R Cairns. Chromatin remodeling: insights and intrigue from single-molecule studies. *Nat Struct Mol Biol*, 14(11):989–996, Nov 2007.
- [2] Anjanabha Saha, Jacqueline Wittmeyer, and Bradley R Cairns. Chromatin remodelling: the industrial revolution of dna around histones. *Nat Rev Mol Cell Biol*, 7(6):437–447, Jun 2006.
- [3] John A Latham and Sharon Y R Dent. Cross-regulation of histone modifications. *Nat Struct Mol Biol*, 14(11):1017–1024, Nov 2007.
- [4] Catherine B Millar and Michael Grunstein. Genome-wide patterns of histone modifications in yeast. *Nat Rev Mol Cell Biol*, 7(9):657–666, Sep 2006.
- [5] Jocelyn E Krebs. Moving marks: dynamic histone modifications in yeast. *Mol Biosyst*, 3(9):590–597, Sep 2007.
- [6] Tony Kouzarides. Chromatin modifications and their function. *Cell*, 128(4):693–705, Feb 2007.
- [7] M. Huss and P. Holme. Currency and commodity metabolites: their identification and relation to the modularity of metabolic networks. *IET Syst Biol*, 1(5):280–285, Sep 2007.
- [8] Julio Collado-Vides and Ralf Hofestädt, editors. *Gene Regulations and Metabolism - Postgenomic Computational Approaches*. MIT Press, 2002.
- [9] Andreas G Ladurner. Rheostat control of gene expression by metabolites. *Mol Cell*, 24(1):1–11, Oct 2006.
- [10] Hidekazu Takahashi, J. Michael McCaffery, Rafael A Irizarry, and Jef D Boeke. Nucleocytosolic acetyl-coenzyme a synthetase is required for histone acetylation and global transcription. *Mol Cell*, 23(2):207–217, Jul 2006.
- [11] Douglas B Murray, Manfred Beckmann, and Hiroaki Kitano. Regulation of yeast oscillatory dynamics. *Proc Natl Acad Sci U S A*, 104(7):2241–2246, Feb 2007.
- [12] R. R. Klevecz and C. M. Li. Evolution of the clock from yeast to man by period-doubling folds in the cellular oscillator. *Cold Spring Harb Symp Quant Biol*, 72:421–429, 2007.
- [13] Robert R Klevecz, James Bolen, Gerald Forrest, and Douglas B Murray. A genomewide oscillation in transcription gates dna replication and cell cycle. *Proc Natl Acad Sci U S A*, 101(5):1200–1205, Feb 2004.
- [14] Douglas B Murray, Robert R Klevecz, and David Lloyd. Generation and maintenance of synchrony in *saccharomyces cerevisiae* continuous culture. *Exp Cell Res*, 287(1):10–15, Jul 2003.
- [15] Ho-Yong Sohn, Eun-Joo Kum, Gi-Seok Kwon, Ingyol Jin, Claire A Adams, and Hiroshi Kuriyama. Glr1 plays an essential role in the homeodynamics of glutathione and the regulation of h2s production during respiratory oscillation of *saccharomyces cerevisiae*. *Biosci Biotechnol Biochem*, 69(12):2450–2454, Dec 2005.
- [16] Caroline M M. Li and Robert R R. Klevecz. A rapid genome-scale response of the transcriptional oscillator to perturbation reveals a period-doubling path to phenotypic change. *Proc Natl Acad Sci U S A*, October 2006.
- [17] Benjamin P. Tu, Andrzej Kudlicki, Maga Rowicka, and Steven L. McKnight. Logic of the yeast metabolic cycle: Temporal compartmentalization of cellular processes. *Science*, 310(5751):1152–1158, 2005.